Examination of the Slow Unfolding of Pro-Nerve Growth Factor Argues against a Loop Threading Mechanism for Nerve Growth Factor†

Marco Kliemannel,‡ Ulrich Weininger,§ Jochen Balbach,§ Elisabeth Schwarz,*,‡ and Rainer Rudolph‡

Institut für Biotechnologie der Martin-Luther-Universität Halle-Wittenberg, Kurt-Mothes-Strasse 3, 06120 Halle, Germany, and Fachbereich Physik, Arbeitsgruppe Biophysik der Martin-Luther-Universität Halle-Wittenberg, Hoher Weg 8, 06099 Halle, Germany

Received September 16, 2005; Revised Manuscript Received January 25, 2006

ABSTRACT: Nerve growth factor (NGF), a member of the neurotrophin family, is an all-β-sheet protein with a characteristic structure motif, the cystine knot. Unfolding of NGF in 6 M GdnHCl has been described previously to involve an initial partial loss of structure and a subsequent very slow conversion to a second, completely unfolded state. This latter conversion was postulated to represent a back-threading of the disulfide bond that passes through the cystine knot (loop threading hypothesis). Here, this hypothesis was questioned with the pro form of the protein (proNGF). In proNGF, the mature part is preceded by the 103-amino acid pro-peptide. Consequently, loop threading of the N-terminally extended protein should be significantly delayed. However, unfolding kinetics of proNGF monitored by RP-HPLC, intrinsic fluorescence, and NMR spectroscopy were comparable to those of mature NGF. Time-resolved $^{1}H-^{15}N$ HSQC spectra revealed a slow time-dependent loss of residual structure of which the kinetics correlated well with the transition observed by RP-HPLC. Refolding from the completely unfolded state led to a partial recovery of natively folded proNGF. In summary, the sequential unfolding of proNGF only marginally differed from that of mature NGF. Therefore, it is very unlikely that a loop threading mechanism is the cause of the slow unfolding step.

NGF[1] belongs to the neurotrophin protein family and promotes growth, maintenance, and differentiation of neurons in the central and peripheral nervous system. NGF conveys its biological activity by binding to the TrkA receptor. The pro form of NGF, proNGF, on the other hand, has been postulated to induce apoptosis via interaction with both p75 and the sortilin receptor (*1*−*5*). NGF is a noncovalent homodimer in which both monomers are tightly associated via hydrophobic interactions. The K_D value for the monomer−dimer equilibrium has been reported to be $\leq 10^{-13}$ M at neutral pH (*6*). NGF, like other neurotrophins, contains a characteristic structure motif, the cystine knot. In NGF, two disulfide bridges connect the polypeptide backbone to a 14-amino acid loop that is penetrated by the third disulfide bridge (*7*−*9*).

In vivo, NGF is translated as a pre-pro-protein. The pre-sequence confers secretion and is cleaved upon translocation into the endoplasmic reticulum where disulfide bond formation occurs. The pro-peptide of NGF with 103 amino acids is nearly as large as the mature part with 118 residues. The pro-peptide is known to promote correct maturation and secretion of NGF in vivo (*10*, *11*). Moreover, we could demonstrate that the pro-peptide of NGF guides effective oxidative folding of the mature protein also in vitro (*12*, *13*). Furthermore, we could show that the mature part stabilizes the pro-peptide (*14*). At low guanidinium hydrochloride (GdnHCl) concentrations, the pro-peptide unfolds fast and does not influence the unfolding of the mature NGF moiety (*14*).

Analysis of structure formation of mouse NGF (the sequence of which is 90% identical with that of human NGF examined here) by unfolding experiments revealed a rapid initial unfolding (*15*, *16*). With longer incubation times under denaturing conditions, murine NGF exhibited a second slow unfolding reaction that resulted in the completely unfolded species (*17*). On the basis of these results, De Young et al. postulated the following sequential unfolding:

$$N_2 \leftrightarrows 2M_1 \leftrightarrows 2M_2$$

The model includes an initial loss of structure, which likely reflects the dissociation of the dimer and partial unfolding to monomer M_1 followed by a slow subsequent complete unfolding to M_2. By NMR measurements, De Young et al. (*17*) analyzed M_1 and concluded that no defined secondary structural elements were retained. However, according to this model, M_1 still contains an intact cystine knot. The transition from M_1 to M_2 was proposed to involve a back-threading of the N-terminal sequence, in which Cys15 is in a disulfide linkage with Cys80, through the ring formed by the other

† This work was supported by Deutsche Forschungsgemeinschaft Grant SCHW 375/4 1-3 (E.S.) and the INTAS-2001 program (J.B.).

* To whom correspondence should be addressed. E-mail: elisabeth.schwarz@biochemtech.uni-halle.de. Phone: +49 345 55 24 856. Fax: +49 345 55 27 013.

‡ Institut für Biotechnologie der Martin-Luther-Universität Halle-Wittenberg.

§ Arbeitsgruppe Biophysik der Martin-Luther-Universität Halle-Wittenberg.

[1] Abbreviations: NGF, nerve growth factor; HSQC, heteronuclear single-quantum correlation; RP-HPLC, reversed phase HPLC; GdnHCl, guanidinium hydrochloride.

10.1021/bi051896t CCC: $33.50
Published on Web 02/21/2006

two disulfides (*17*, *18*). Accordingly, M_2 was assumed to represent an unfolded species in which the N-terminal sequence has slipped out of the ring (*17*). A gain in entropy was suggested as the driving force for threading. A rearrangement of disulfide bonds, as an alternative explanation for the slow conversion, was excluded since unfolding was independent of pH. The loop threading hypothesis was supported by the observation that NGF variants with truncated N-termini underwent the transition from M_1 to M_2 considerably faster (*17*). In proNGF, the mature part is preceded by the pro-peptide comprising 103 amino acids. Accordingly, threading through the ring should be significantly retarded in proNGF. Here, we compare the folding and unfolding of proNGF with that of mature NGF. Our results show that the N-terminal pro-peptide has no influence on the slow M_1 to M_2 conversion. Furthermore, NMR experiments revealed new insight into the structural differences between the M_1 and M_2 states. Taken together, our results suggest that the M_1 and M_2 states differ in the residual structure in the M_1 state probably close to the cystine knot.

MATERIALS AND METHODS

Preparation of Recombinant Human proNGF and NGF. Inclusion bodies of human proNGF were produced with pET11a in *Escherichia coli* BL21(DE3), and the fully folded protein was obtained as described previously (*12*). Mature NGF was obtained from proNGF by digestion with bovine pancreatic trypsin (Roche) (1:415 molar ratio). After a 30 min digestion in 50 mM Tris-HCl (pH 8.0) at 0 °C, trypsin and cleavage products were removed by ion exchange chromatography on a SP-Sepharose column (GE Healthcare) (*12*).

NMR Spectroscopy. For ^{15}N labeling of *E. coli* BL21(DE3) cells containing recombinant cDNA for proNGF, cells were cultured in M9 medium with $^{15}NH_4Cl$ as the sole nitrogen source. Proton spectra of 0.435 mM proNGF samples and 1 mM uniformly ^{15}N-labeled NGF samples were acquired at 45 °C with a Bruker DRX 500 spectrometer. The residual water resonance in the D_2O samples of the unfolding buffer, containing 6 M GdnHCl and 50 mM sodium phosphate (pH 7.0), was presaturated during the relaxation delay. Due to the fast exchange of water and GdnHCl protons and thus the complete saturation transfer to the GdnHCl resonance at 45 °C, an additional suppression of the denaturant was not necessary. The concentration of GdnHCl was determined by refraction without correction for the isotopic effect of D_2O. Exchangeable protons of the buffer were removed by dissolving the sample in D_2O three times and subsequent lyophilization. Unfolding reactions were started by manually dissolving the lyophilized protein in the unfolding buffer. The unfolding kinetics of proNGF were measured in D_2O (6 M GdnDCl and 50 mM sodium phosphate, pD 7.0 pH-meter reading), recording 800 one-dimensional (1D) ^1H spectra (64 scans each) over 19 h. Spectra were recorded over a spectral width of 13 ppm. A squared cosine window function was applied prior to Fourier transformation. The unfolding of ^{15}N-NGF was followed via 28 $^1H-^{15}N$ HSQC spectra over 24 h in 6 M GdnHCl (90% H_2O/10% D_2O). The spectral widths for the HSQC spectra were 13 and 32 ppm for the ^1H and ^{15}N dimensions, respectively. Quadrature detection in the indirect dimension was achieved using the States−TPPI method. The GdnHCl signal was suppressed by a 1 s presaturation and the water signal by the WATERGATE pulse train of the FHSQC sequence (*19*).

Data were processed and analyzed using Felix. The 1D spectra depicted in Figure 4A are averages of 100 1D spectra. The spectrum of M_2 was recorded after the unfolding reaction had reached completion. For the M_1 state, the first 100 1D spectra during refolding were averaged. According to the unfolding kinetics, 75% of this average NMR intensity belongs to M_2. Therefore, after subtraction of these 75% using the plain M_2 spectrum recorded after the unfolding reaction, the 1D spectrum of M_1 could be derived. For more details about this deconvolution of 1D real-time NMR spectra, see refs *20* and *21*. The two-dimensional (2D) HSQCs of M_1 and M_2 were derived by the similar approach using averages of five spectra.

For the kinetic studies, the high-field-shifted methyl groups of the proNGF 1D ^1H spectra between 0.3 and 0.6 ppm were integrated and plotted against the unfolding time. For the analysis of the 2D HSQC, the intensities of the amide cross-peaks were followed. Kinetic analyses were performed using GraFit (Erithacus Software Ltd.).

Reversed Phase High-Pressure Liquid Chromatography (RP-HPLC). RP-HPLC was performed with a C4-RP-HPLC column (Vydac, C4, 5 μm; 4.6 mm × 250 mm; Hesperia) on a Gynkotek HPLC system (Dionex, Idstein, Germany). The samples were loaded after incubation at different temperatures and time points. The column was equilibrated in 6% buffer B [buffer A was 0.1% (v/v) TFA in water; buffer B was 80% (v/v) acetonitrile and 0.08% (v/v) TFA in water]. Samples were eluted with the following gradient: 6% B from 0 to 4 min, 6 to 30% B from 4 to 9 min, 30 to 69% B from 9 to 24 min, and 69 to 100% B from 24 to 25 min at a flow rate of 1 mL/min. Peak areas were calculated with Chromeleon version 4.32 (Dionex).

Circular Dichroism (CD) Measurements. Far-UV CD spectra were recorded on a Jasco J710 spectropolarimeter from 190 to 260 nm with a 1 nm light path. Measurements were performed in 50 mM sodium phosphate (pH 7.0) at 20 °C. Spectra were buffer corrected, and ellipticities related to the mean residue weight of amino acid residues were calculated according to the method described in ref *22*.

Fluorescence Measurements. Measurements were carried out with a FluoroMax-2 fluorescence spectrometer (Jobin-Yvon-Spex). Slit widths for both excitation and emission wavelengths were 5 nm. Experiments were performed in 50 mM sodium phosphate (pH 7.0) and 1 mM EDTA at 20 °C in 1 cm cuvettes. For emission spectra, excitation was at 280 nm. Spectra were collected from 300 to 400 nm. Kinetics were recorded upon excitation at 280 nm and by monitoring emission at 325 nm in 1 cm cuvettes with stirring.

Refolding of ProNGF from the M_2 State. Fully unfolded proNGF (6 M GdnHCl at 45 °C over 4 days) was refolded by pulse renaturation in 50 mM sodium phosphate (pH 7.0) and 1 mM EDTA. The protein concentration of each pulse was 200 μg/mL. ProNGF was refolded in five pulses over 120 h, and the final residual concentration of GdnHCl was 0.2 M.

Gel Filtration. For separation of dimeric species from monomeric species, size exclusion chromatography was performed on a Superdex75 10/300 column with the ÄKTA explorer system (Amersham Biosience) at a flow rate of 0.5

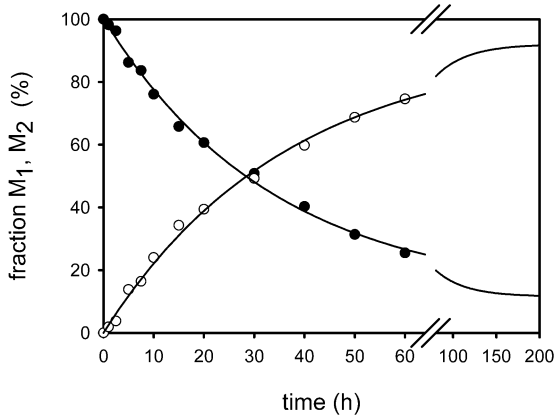

FIGURE 1: Unfolding kinetics of NGF. NGF (300 μg/mL) was incubated in 6 M GdnHCl, 50 mM sodium phosphate (pH 7.0), and 1 mM EDTA at 25 °C. At different time points, 30 μg of protein was loaded on a C4-RP-HPLC column: (●) proNGF in the M_1 state and (○) NGF in the M_2 state. Rate constants were calculated by integration of peak areas and by assuming a first-order reaction ($k = 0.029$ h^{-1}).

mL/min. The mobile phase consisted of 0.33 M L-arginine, 50 mM sodium phosphate (pH 7.0), and 1 mM EDTA.

RESULTS AND DISCUSSION

Influence of the Pro-Peptide on the Unfolding Kinetics of the Mature Domain. The kinetics of NGF unfolding upon denaturation with GdnHCl were studied in detail by De Young et al. (*17*, *18*). The authors separated the partially unfolded monomeric species, M_1, from the fully denatured species, M_2, that eluted at higher acetonitrile concentrations than M_1 on a C4-RP-HPLC column. As performed by De Young et al., conversion of M_1 to M_2 was quantified here by the integration of peak areas. Conversion of M_1 to M_2 during RP-HPLC analysis can be excluded, since rechromatography of the M_1 and M_2 species via RP-HPLC did not result in changes in the elution properties of either species (data not shown). The results of De Young et al. could be confirmed in our lab by identical analyses. The rate constant (k) for the M_1 to M_2 transition equaled 0.029 h^{-1} and was thus very similar to that determined by De Young et al. (0.03 h^{-1}) (Figure 1).

The loop threading hypothesis is supported by the observation that rate constants of dimer loss increased with longer deletions of N-terminal segments in mutant variants of NGF (*17*). Accordingly, N-terminal extensions of NGF should lead to severely retarded conversions of M_1 to M_2. To this end, unfolding kinetics of proNGF, in which the mature part is preceded by the 103-residue pro-peptide, were measured. Experimental conditions were identical to those in the studies with mature NGF. GdnHCl-induced unfolding of native proNGF to M_1, which is supposed to be coupled with the dissociation of the dimer, was monitored by fluorescence. At 20 °C, the fast unfolding reaction (N to M_1) was complete after 2 min (Figure 2A). Conversion of M_1 to M_2 was monitored by RP-HPLC. Due to the fast unfolding of the pro-peptide, which is already at low GdnHCl concentrations in the millisecond range (data not shown), an influence of any residual structure(s) in the pro-peptide on the transition of M_1 to M_2 could be excluded.

In proNGF, conversion of M_1 to M_2 occurred with a rate constant k of 0.024 h^{-1} (Figure 2B). The rate of conversion

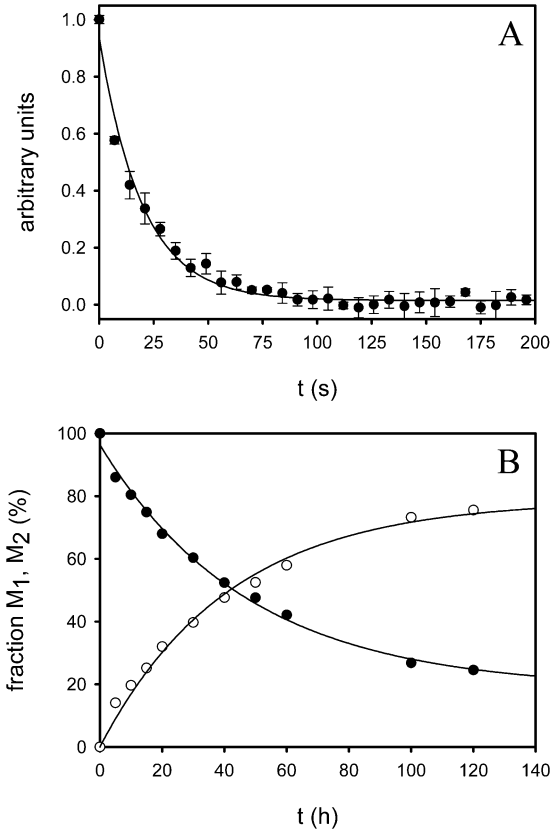

FIGURE 2: (A) Unfolding kinetics of proNGF from the native to the M_1 state. ProNGF (20 μg/mL) was incubated in 6 M GdnHCl, 50 mM sodium phosphate (pH 7.0), and 1 mM EDTA. The fluorescence was measured at 20 °C at 325 nm upon excitation at 280 nm. The decay of the signal was fitted to a first-order reaction ($k = 0.04$ s^{-1}). (B) Unfolding kinetics of proNGF from the M_1 state to the M_2 state. ProNGF (10 μg) was incubated in 6 M GdnHCl, 50 mM sodium phosphate (pH 7.0), and 1 mM EDTA. After different incubation intervals, samples were loaded onto a C4-RP-HPLC column: (●) proNGF in the M_1 state and (○) proNGF in the M_2 state. Rate constants were calculated by integration of peak areas and by subsequently assuming a first-order reaction ($k = 0.024$ h^{-1}).

was independent of the pH (data not shown), excluding the possibility of disulfide rearrangements. The determined rate constant is very close to that of the corresponding reaction of mature NGF ($k = 0.029$ h^{-1}). Thus, it is unlikely that the slow unfolding reaction that is observed in both NGF and proNGF is caused by a loop threading mechanism since in the case of proNGF considerably longer unfolding rates for the threading of the 103-amino acid pro-peptide would be expected.

Temperature-Dependent Unfolding of ProNGF. Proline isomerizations with activation energies of 75−91 kJ/mol (*23*) are known to cause slow unfolding reactions. However, a higher energy barrier of 108−112 kJ/mol was calculated from temperature-dependent conversion of M_1 to M_2 in NGF by De Young et al. (*17*). On the basis of these results, the authors excluded proline isomerization(s) as a reason for the slow unfolding. To characterize the activation energies of proNGF unfolding, rate constants were determined at various temperatures (Figure 3A and Table 1). For the slow M_1 to M_2 transition, an activation enthalpy ($\Delta H^{\ddagger}$) of 88.8 ± 5.3 kJ/mol and an entropy ($\Delta S^{\ddagger}$) of 20.5 ± 2.0 J mol^{-1} K^{-1}, resulting in a $\Delta G^{\ddagger}$ of 82.8 ± 6.6 kJ/mol at 20 °C, were calculated (Figure 3B). This considerably smaller $\Delta G^{\ddagger}$ value,

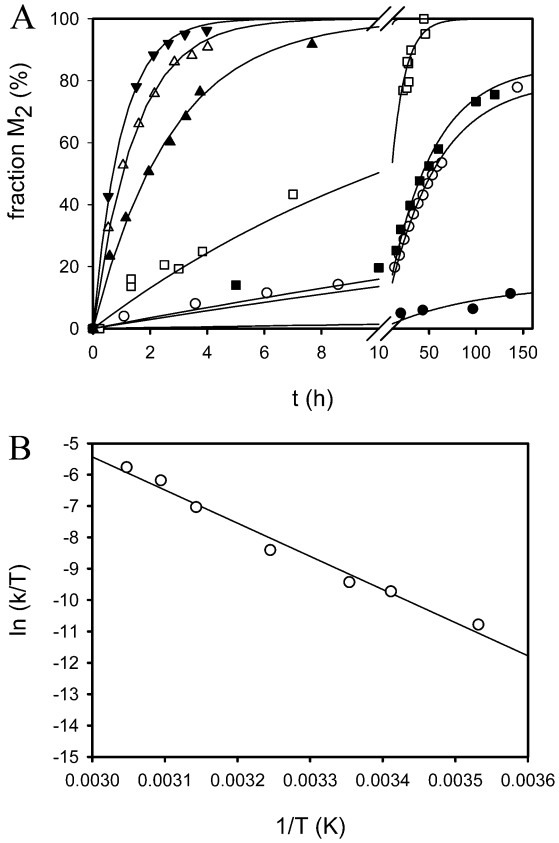

FIGURE 3: (A) Temperature dependence of the M_1 to M_2 transition of proNGF. Protein (10 μg/mL) was incubated in 6 M GdnHCl, 50 mM sodium phosphate (pH 7.0), and 1 mM EDTA: (●) 10, (○) 20, (■) 25, (□) 35, (▲) 45, (△) 50, and (▼) 55 °C. Resulting rate constants (Table 1) were derived by a first-order reaction. (B) Arrhenius plot of the rate constants.

Table 1: Temperature Dependence of the Apparent First-Order Rate Constants for the Conversion of M_1 to M_2

temp (°C)	k_{obs} (h^{-1})	temp (°C)	k_{obs} (h^{-1})
10	0.0053 ± 0.001	45	0.28 ± 0.025
20	0.0176 ± 0.004	50	0.67 ± 0.037
25	0.024 ± 0.0018	55	1.03 ± 0.015
35	0.069 ± 0.008		

compared to that determined by De Young et al., corresponds to the observed activation energies of proline isomerizations. A possible influence of the pro-peptide on the $\Delta G^{\ddagger}$ of the mature part is very unlikely, since a small stabilization energy (ΔG^0) of −7.8 kJ/mol for the pro-peptide had been determined previously (*14*). Thus, proline isomerization(s) accounting for the slow unfolding can presently not be excluded on the basis of the thermodynamic results.

1D NMR Studies of ProNGF in the M_1 State and the Transition to M_2. For a more detailed investigation of the M_1 state of proNGF in terms of residual structure, a time-resolved 1D NMR experiment was performed (*24*). Unfolding at 45 °C was induced by dissolving a lyophilized sample of proNGF to a final protein concentration of 1 mM in D_2O containing 6 M GdnDCl. During the dead time of ∼15 min for this experiment, native species were no longer populated. Each of the 800 1D NMR spectra, recorded after the unfolding reactions had been started, contained a superposition of the M_1 and M_2 state. Deconvolution of this real-time NMR data set as described previously (*20*, *21*) revealed the

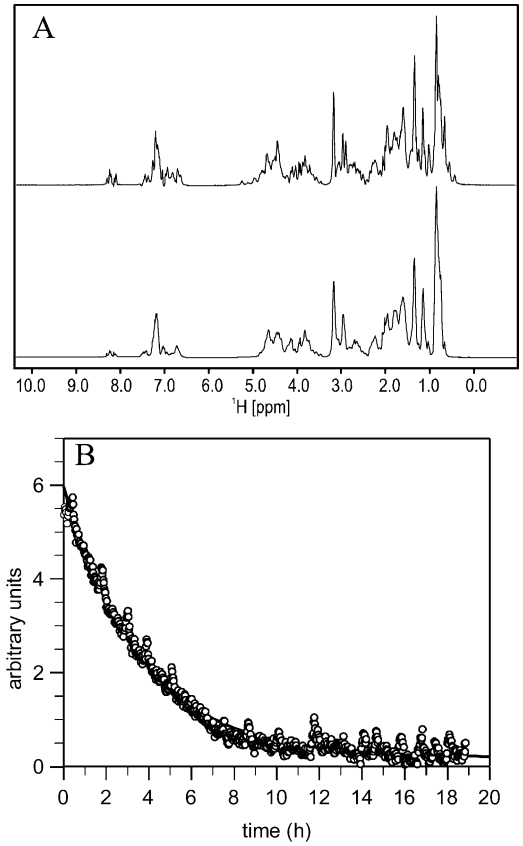

FIGURE 4: (A) 1D NMR spectra of proNGF in the M_1 state (top) and the M_2 state (bottom) at 45 °C in 6 M GdnDCl and 50 mM sodium phosphate (pD 7) in 100% D_2O. The top spectrum of the kinetic intermediate was derived from deconvoluting the 1D real-time NMR data according to the unfolding kinetics. (B) Decrease in the NMR integral of the high-field-shifted methyl groups between 0.3 and 0.6 ppm upon unfolding in 6 M GdnDCl. The solid line represents a fit of a single-exponential function to the NMR intensity resulting in a rate constant of 0.28 ± 0.01 h^{-1} at 45 °C.

1D spectrum of M_1 (Figure 4A, top spectrum) and M_2 (Figure 4A, bottom spectrum). The 1D NMR spectrum of M_2 shows the characteristic dispersion of a completely unfolded polypeptide chain without secondary or tertiary interactions. In contrast, the 1D spectrum of the M_1 state revealed some high-field-shifted side chain resonances below 0.7 ppm and several low-field-shifted H^{α} resonances between 4.8 and 5.2 ppm, which are indicative of residual structure. The resonances of nonexchangeable protons from the 26 aromatic side chains are located between 6.5 and 7.5 ppm, and those of the $H^{\epsilon 1}$ protons of the nine histidine residues were between 8.0 and 8.5 ppm. These resonances have a low dispersion in both the M_1 and M_2 states, indicating an unfolded conformation. All 26 aromatic residues are well distributed along the primary sequence, and only Tyr79 is close to the cystine knot in the three-dimensional structure (*8*). Therefore, it is likely that only a local residual structure is preserved around the cystine knot in M_1, which cannot be unambiguously resolved by 1D NMR spectroscopy.

The high-field-shifted NMR signals were used to determine the unfolding kinetics for the transition from the M_1 state to the M_2 state. A single-exponential function has been fitted to the decay of the integral between 0.3 and 0.6 ppm during the 19 h monitoring as depicted in Figure 4B. The unfolding rate constant (k) of 0.28 ± 0.01 h^{-1} at 45 °C in D_2O at NMR concentration is identical to the rate

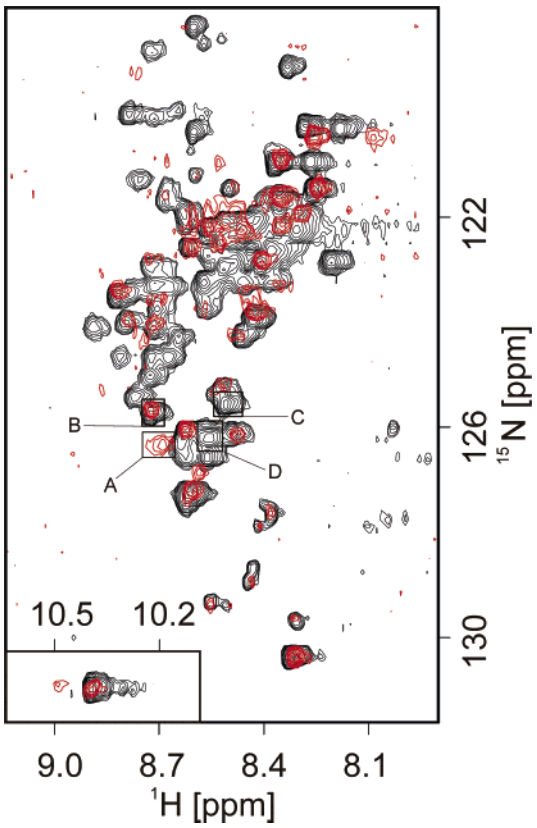

FIGURE 5: ^{1}H−^{15}N HSQC spectra of uniformly ^{15}N-labeled NGF in 6 M GdnHCl at 45 °C. The spectrum of completely unfolded NGF (M_2 state) is colored black, and the spectrum of the intermediate M_1 state derived after deconvolution of the 2D real-time NMR experiment is colored red. Cross-peaks, for which a kinetic analysis is provided in Figure 6, are denoted with boxes (A−D). The inset shows the horizontally shifted side chain resonances of Trp.

constant observed by the HPLC approach at 45 °C (0.28 h^{-1}) (Figure 3A).

2D NMR Studies for the M_1 State and the Transition to M_2 of NGF. Unfolding of mature NGF has been studied by 1D real-time NMR (*17*). To increase the resolution of the NMR spectra, unfolding of uniformly labeled ^{15}N-NGF at 45 °C in 6 M GdnHCl was monitored by a set of 28 2D ^{1}H−^{15}N HSQC spectra over 24 h. These 2D spectra again contained cross-peaks of the M_1 and M_2 states, which could be deconvoluted via unfolding kinetics (*20*, *21*). The result is plotted in Figure 5. Black contours represent the cross-peaks of M_2, which is simply the last 2D spectrum recorded after completion of the unfolding reaction. Red resonances result from the amides of the M_1 state. The cross-peaks around 10 ppm originate from the $H^{\epsilon 1}$ protons of the three tryptophan side chains of NGF (inset of Figure 5). Their chemical shifts and intensities match exactly those of the reported 1D spectrum of the M_1 and M_2 states (*17*), confirming the reproducibility of these real-time NMR experiments.

The most prominent cross-peaks of the backbone and side chain amides of M_1 (red in Figure 5) are located at chemical shifts, where M_2 shows resonances as well. The few exceptions are the already mentioned $H^{\epsilon 1}$ proton of three tryptophan side chains, the cross-peak marked by box A in Figure 5, and some side chain resonances between 120 and 122 ppm. They indicate not completely unfolded regions in M_1. All other observable signals of M_1 originate from completely unfolded stretches of the polypeptide chain. These signals exhibited constant intensities during the entire unfolding experiment. One representative time course is shown in Figure 6B for the resonance indicated by box B in Figure 5. The striking observation was that at least 50% of the backbone amide cross-peaks in the 2D HSQC spectrum of M_1 were missing probably due to chemical exchange broadening. The appearance of the 2D HSQC spectra of NGF resembles closely that of spectra of other folding intermediates such as the molten globule of α-lactalbumin. In this case, both for the pH 2 state at equilibrium and for the kinetic molten globule under refolding conditions, the majority of cross-peaks were missing (*25*, *26*). A molten globule-like structure of M_1, however, is unlikely since, for example, the far-UV CD spectra of M_1 and M_2 are superimposable (data not shown).

The time dependence of the intensities of those cross-peaks of M_2, which do not overlap with resonances of M_1, revealed uniform unfolding rates. Seventeen signals could be analyzed with an average unfolding rate k of 0.28 ± 0.03 h^{-1}. Two of these kinetics are shown in panels C and D of Figure 6. They were derived from cross-peaks marked by boxes C and D in Figure 5. The decay of M_1 (Figure 6A) could be monitored by the signal in box A, giving a rate constant k of 0.29 ± 0.05 h^{-1}. These coinciding rate constants monitored by reporters of the M_1 and M_2 state indicate that no further, detectable kinetic intermediate is populated during the M_1 to M_2 transition.

Characterization of the Structural Differences of the M_1 and M_2 States. Three experimental observations verify structural differences between M_1 and M_2. First, both states can be separated by RP-HPLC. Second, differences in the dispersion of the ^{1}H resonances in the 1D spectra exist. Third, missing cross-peaks in the 2D HSQC spectrum of M_2 were observed. However, far-UV CD spectroscopy of the two states revealed no differences in the secondary structure level (data not shown). To gain further insight into the structural differences between the two states, the kinetics of reduction of M_1 and M_2 species were monitored by RP-HPLC (Figure 7). Reduction with 100 mM DTT was 30 times faster with M_2 than with M_1, pointing to a better accessibility of the disulfides in M_2. Accordingly, the residual structure in the M_1 species is most likely close to the cystine knot, preventing fast reduction even in 6 M GdnHCl. We suggest that the integrity of this residual structure in M_1 presents a nucleation structure enabling the much faster and more complete refolding from M_1 than from M_2 in both mature mouse NGF (*16*) and human proNGF (data not shown).

Renaturation of ProNGF from the M_2 State. If M_2 species would represent species in which the N-terminus had threaded out of the cystine knot, the reverse reaction, i.e., refolding of proNGF, would be inhibited. Therefore, we analyzed the time-dependent renaturation of proNGF starting from the M_2 state. For quantification of refolding kinetics from M_2, the fully denatured protein was refolded by dialysis against refolding buffer. However, refolding of proNGF at high protein concentrations (>60 μM) was accompanied by aggregation. Thus, to suppress aggregation, refolding was initiated by rapid dilution of small amounts of denatured protein into refolding buffer to final concentrations of approximately 8 μM. Refolding was monitored by RP-HPLC,

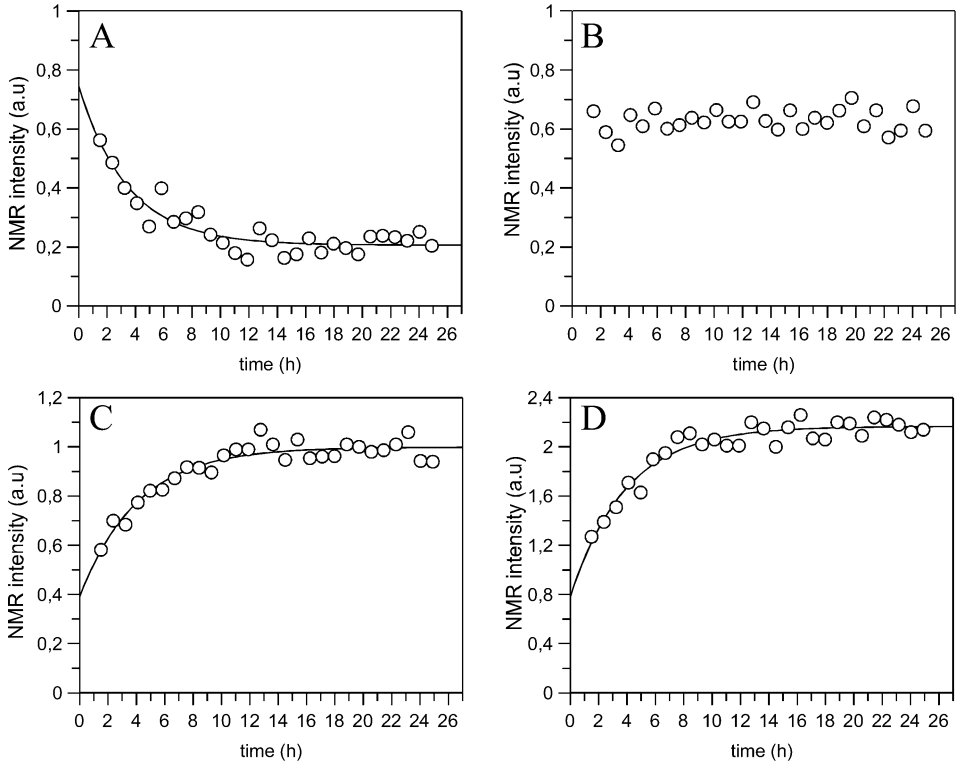

FIGURE 6: Time-dependent intensities of the four cross-peaks indicated in the 2D HSQC spectra of NGF recorded during the unfolding reaction. Single-exponential fits are given as solid lines. (A) Decay of the M_1 state with a rate constant of 0.29 ± 0.05 h^{-1}. (B) Invariant NMR intensity with unfolding time. (C and D) Increase in the level of of the M_2 state with rate constants of 0.27 ± 0.03 and 0.26 ± 0.04 h^{-1}, respectively.

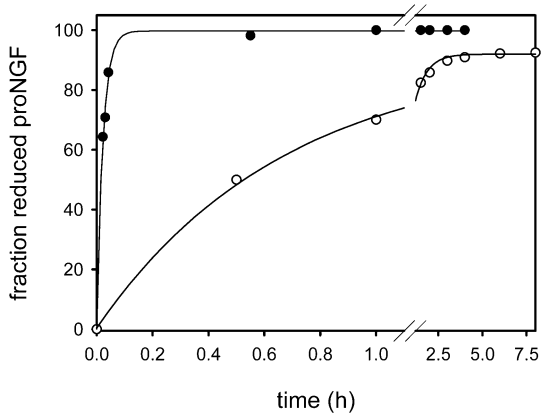

FIGURE 7: Kinetics of reduction of proNGF in the M_1 (○) and M_2 state (●) in 100 mM DTT, 6 M GdnHCl, 50 mM sodium phosphate, and 1 mM EDTA (pH 7.0) at 20 °C. Quantification of M_1, M_2, and the reduced species was performed as described in Materials and Methods by RP-HPLC.

a method that allows differentiation between only M_2 and M_1, since under the HPLC buffer conditions native protein is immediately converted to M_1 (*17*). However, since M_1 is in rapid equilibrium with native species, the technique is suitable for monitoring refolding from M_2 (*17*) (Figure 8A).

With a prolonged incubation under refolding conditions, the peak area representing M_2 gradually decreased (Figure 8A). Concomitantly, the earlier eluting peak representing M_1 species increased. From the peak areas, the ratios of the two folding species were calculated. The decrease in the amount of M_2 and the increase in the amount of refolded species were analyzed as a first-order reaction (Figure 8B). A rate constant k of 0.083 h^{-1} was determined. The yield of conversion was 75%. The sum of both peaks correlated with the total protein concentration, indicating that no aggregation had taken place during the refolding reaction.

To confirm that natively folded protein had been obtained, the refolded species were analyzed by fluorescence, far-UV CD spectroscopy, and analytical ultracentrifugation. All analyses revealed inhomogeneous protein populations (data not shown). Hence, it was necessary to further purify the native species. Since only a dimeric species is supposed to represent the correctly folded conformation, purification was based on the separation of the dimeric species from monomeric species by size exclusion chromatography (*6*, *16*). The far-UV CD spectrum of the purified dimeric protein was almost superimposable with that of native proNGF (Figure 9A). Furthermore, the fluorescence spectra of the refolded protein and the reference, native proNGF, were nearly identical (Figure 9B). These results demonstrate that proNGF refolded from M_2 contains the same secondary and tertiary structure elements as the starting material. Further analysis by analytical ultracentrifugation demonstrated the dimeric state (data not shown) as already shown for native proNGF (*12*).

For quantification of the refolding yields, peak areas of the dimeric species obtained by SEC were calculated. A total yield of ca. 30% native proNGF was determined (data not shown). A refolding yield of 30% did not correlate with that determined by RP-HPLC (peak areas representing M_1) (75%) (Figure 9B). This indicates that the M_1 peak also contains besides native proNGF unproductive folding intermediates, which resemble under RP-HPLC conditions the M_1 state. Native proNGF obtained upon refolding of M_2 was additionally analyzed by unfolding kinetics. Here, the refolded protein without subsequent purification was tested. Unfolding was

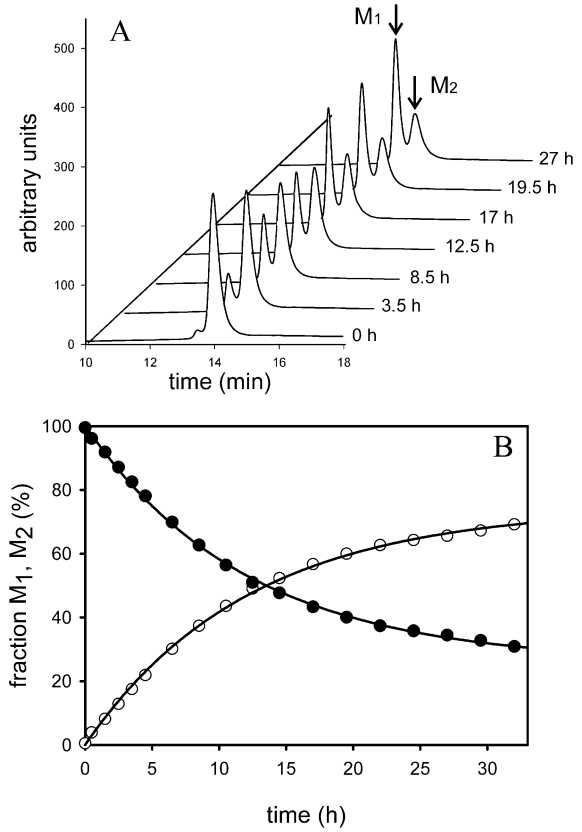

FIGURE 8: Refolding of proNGF from the M_2 state. Refolding was performed at a concentration of 200 μg/mL in 50 mM sodium phosphate (pH 7.0) and 1 mM EDTA at 20 °C (residual GdnHCl concentration of 35 mM). At different time points, aliquots were withdrawn and analyzed by RP-HPLC. (A) RP-HPLC chromatograms during refolding of proNGF from the M_2 state. (B) Refolding kinetics monitored by RP-HPLC. Peak areas of M_1 (○) and M_2 (●) were fitted to a first-order reaction ($k = 0.083$ h^{-1}).

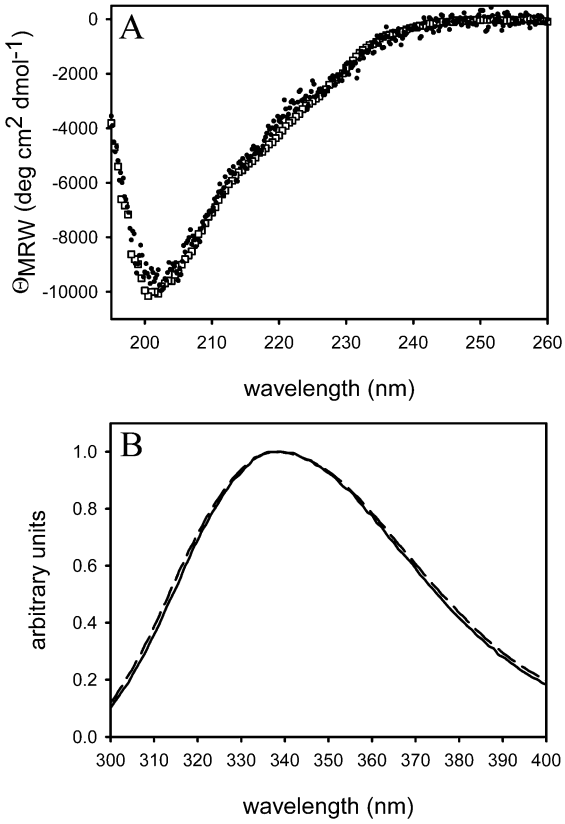

FIGURE 9: (A) Far-UV CD spectra of proNGF (0.55 mg/mL) in 50 mM sodium phosphate (pH 7.0) in a 0.5 mm cuvette at 20 °C: (□) M_2-refolded proNGF and (●) native proNGF. (B) Fluorescence spectra (10 μg/mL) in 50 mM sodium phosphate (pH 7.0) and 1 mM EDTA upon excitation at 280 nm: (—) M_2-refolded proNGF and (– – –) native proNGF.

induced by chemical denaturation with GdnHCl and monitored by fluorescence spectroscopy. The same unfolding rate constant was observed as with the reference, but only ca. 30% of the expected amplitude, a finding that corresponded well with the renaturation yield of 30% determined before by gel filtration.

NGF contains three proline residues: Pro5, Pro61, and Pro63. The crystal structure of Pro5 shows a trans conformation (*8*). The states of Pro61 and Pro63 are located in the loop region of the cystine knot, which is not resolved in cocrystallizations of NGF with either TrkA or p75 (*8*, *9*). The crystal structure of mouse NGF, which contains one conserved proline residue in the cystine knot, reveals that this prolyl bond is also in the trans conformation (*7*). To test whether slow unfolding may reflect cis−trans isomerization(s) of one or more proline residues, several well-known proline isomerases, cyclophilin 12, FKPB 18, and SlyD, were tested for their ability to accelerate the refolding rate. None of the isomerases resulted in an acceleration of the refolding reaction of proNGF (data not shown). Nevertheless, proline isomerization(s) as a reason for the very slow refolding kinetics cannot be fully ruled out since the accessibility of the isomerases to the proline residues may be sterically hindered.

Several lines of evidence have been collected in this work that argue against a loop threading mechanism that has been postulated to underlie the slow unfolding of NGF. First, the pro-peptide of NGF does not significantly retard the transition from M_1 to M_2. A retarded unfolding would have been expected if loop threading were occurring since then the longer N-terminal sequence would require more time to slip through the ring. Second, the M_2 state of proNGF can be refolded to the native form. Refolding to the native conformation with a yield of 30% cannot be reconciled with loop threading, since the N-terminal sequence would first have to find the ring and then have to pass through it. Third, NMR analyses showed in the M_1 state residual structures. Loop threading would predict that M_1 and M_2 differ only by a not yet slipped N-terminal sequence through the cystine knot of the fully unfolded polypeptide chain. Therefore, the NMR spectra of both NGF and proNGF in the M_2 and M_1 states should be almost identical, which was not the case. Fourth, the residual structure in M_1 which is most likely located close to the cystine knot is probably responsible for the slow unfolding.

Recently, an unfolding intermediate possibly similar to M_1 was described for FGF-1 from newt (nFGF), an all-β-sheet growth factor devoid of disulfide bonds (*27*). Renaturation from the intermediate state was almost fully reversible. Prolonged incubation under denaturing conditions led eventually to complete unfolding because renaturation from this second state was incomplete. The authors interpreted the slow unfolding as a final rearrangement of a hydrophobic core. This description of another slow unfolding protein lacking disulfide bridges and the results presented here render a loop threading mechanism very unlikely. Rather, evidence that

NGF and proNGF may unfold via a partially structured intermediate was collected. Since neurotrophins share a high degree of sequence and structure homology, presumably, loop threading may not underlie the slow unfolding of the other members of this family.

ACKNOWLEDGMENT

We thank Gunter Fischer, Christian Lücke, and Monika Seidel at the Max-Planck research unit for enzymology of protein folding for the NMR time and assistance. We thank Hauke Lilie for helpful suggestions.

REFERENCES

1. Levi-Montalcini, R. (1987) The nerve growth factor 35 years later, *Science 237*, 1154−1162.
2. Hefti, F. (1994) Neurotrophic factor therapy for nervous system degenerative diseases, *J. Neurobiol. 25*, 1418−1435.
3. Casaccia-Bonnefil, P., Carter, B. D., Dobrowsky, R. T., and Chao, M. V. (1996) Death of oligodendrocytes mediated by the interaction of nerve growth factor with its receptor p75, *Nature 383*, 716−719.
4. Frade, J. M., Rodriguez-Tebar, A., and Barde, Y. A. (1996) Induction of cell death by endogenous nerve growth factor through its p75 receptor, *Nature 383*, 166−168.
5. Nykjaer, A., Lee, R., Teng, K. K., Jansen, P., Madsen, P., Nielsen, M. S., Jacobsen, C., Kliemannel, M., Schwarz, E., Willnow, T. E., Hempstead, B. L., and Petersen, C. M. (2004) Sortilin is essential for proNGF-induced neuronal cell death, *Nature 427*, 843−848.
6. Bothwell, M. A., and Shooter, E. M. (1977) Dissociation equilibrium constant of β nerve growth factor, *J. Biol. Chem. 252*, 8532−8536.
7. McDonald, N. Q., Lapatto, R., Murray-Rust, J., Gunning, J., Wlodawer, A., and Blundell, T. L. (1991) New protein fold revealed by a 2.3-Å resolution crystal structure of nerve growth factor, *Nature 354*, 411−414.
8. Wiesmann, C., Ultsch, M. H., Bass, S. H., and de Vos, A. M. (1999) Crystal structure of nerve growth factor in complex with the ligand-binding domain of the TrkA receptor, *Nature 401*, 184−188.
9. He, X. L., and Garcia, K. C. (2004) Structure of nerve growth factor complexed with the shared neurotrophin receptor p75, *Science 304*, 870−875.
10. Suter, U., Heymach, J. V., Jr., and Shooter, E. M. (1991) Two conserved domains in the NGF propeptide are necessary and sufficient for the biosynthesis of correctly processed and biologically active NGF, *EMBO J. 10*, 2395−2400.
11. Seidah, N. G., Benjannet, S., Pareek, S., Savaria, D., Hamelin, J., Goulet, B., Laliberte, J., Lazure, C., Chretien, M., and Murphy, R. A. (1996) Cellular processing of the nerve growth factor precursor by the mammalian pro-protein convertases, *Biochem. J. 314*, 951−960.
12. Rattenholl, A., Lilie, H., Grossmann, A., Stern, A., Schwarz, E., and Rudolph, R. (2001) The pro-sequence facilitates folding of human nerve growth factor from *Escherichia coli* inclusion bodies, *Eur. J. Biochem. 268*, 3296−3303.
13. Rattenholl, A., Ruoppolo, M., Flagiello, A., Monti, M., Vinci, F., Marino, G., Lilie, H., Schwarz, E., and Rudolph, R. (2001) Pro-sequence assisted folding and disulfide bond formation of human nerve growth factor, *J. Mol. Biol. 305*, 523−533.
14. Kliemannel, M., Rattenholl, A., Golbik, R., Balbach, J., Lilie, H., Rudolph, R., and Schwarz, E. (2004) The mature part of proNGF induces the structure of its pro-peptide, *FEBS Lett. 566*, 207−212.
15. Ullrich, A., Gray, A., Berman, C., and Dull, T. J. (1983) Human β-nerve growth factor gene sequence highly homologous to that of mouse, *Nature 303*, 821−825.
16. Timm, D. E., and Neet, K. E. (1992) Equilibrium denaturation studies of mouse β-nerve growth factor, *Protein Sci. 1*, 236−244.
17. De Young, L. R., Burton, L. E., Liu, J., Powell, M. F., Schmelzer, C. H., and Skelton, N. J. (1996) RhNGF slow unfolding is not due to proline isomerization: Possibility of a cystine knot loop-threading mechanism, *Protein Sci. 5*, 1554−1566.
18. De Young, L. R., Schmelzer, C. H., and Burton, L. E. (1999) A common mechanism for recombinant human NGF, BDNF, NT-3, and murine NGF slow unfolding, *Protein Sci. 8*, 2513−2518.
19. Mori, S., Abeygunawardana, C., Johnson, M. O., and van Zijl, P. C. (1995) Improved sensitivity of HSQC spectra of exchanging protons at short interscan delays using a new fast HSQC (FHSQC) detection scheme that avoids water saturation, *J. Magn. Reson., Ser. B 108*, 94−98.
20. Balbach, J., Steegborn, C., Schindler, T., and Schmid, F. X. (1999) A protein folding intermediate of ribonuclease T1 characterized at high resolution by 1D and 2D real-time NMR spectroscopy, *J. Mol. Biol. 285*, 829−842.
21. Zeeb, M., Rosner, H., Zeslawski, W., Canet, D., Holak, T. A., and Balbach, J. (2002) Protein folding and stability of human CDK inhibitor p19(INK4d), *J. Mol. Biol. 315*, 447−457.
22. Schmid, F. X. (1997) Spectral methods of characterizing protein conformation and conformational changes, in *Protein structure: A practical approach* (Creighton, T. E., Ed.) 1st ed., pp 251−286, IRL-Press, Oxford University Press, Oxford, U.K.
23. Schmid, F. X., and Baldwin, R. L. (1979) The rate of interconversion between the two unfolded forms of ribonuclease A does not depend on guanidinium chloride concentration, *J. Mol. Biol. 133*, 285−287.
24. Balbach, J., Forge, V., van Nuland, N. A., Winder, S. L., Hore, P. J., and Dobson, C. M. (1995) Following protein folding in real time using NMR spectroscopy, *Nat. Struct. Biol. 2*, 865−870.
25. Balbach, J., Forge, V., Lau, W. S., van Nuland, N. A., Brew, K., and Dobson, C. M. (1996) Protein folding monitored at individual residues during a two-dimensional NMR experiment, *Science 274*, 1161−1163.
26. Schulman, B. A., Kim, P. S., Dobson, C. M., and Redfield, C. (1997) A residue-specific NMR view of the non-cooperative unfolding of a molten globule, *Nat. Struct. Biol. 4*, 630−634.
27. Kathir, K. M., Kumar, T. K., Rajalingam, D., and Yu, C. (2005) Time-dependent changes in the denatured state(s) influence the folding mechanism of an all β-sheet protein, *J. Biol. Chem. 280*, 29682−29688.

BI051896T